SUPPLEMENTAL MATERIAL

Survivin-induced abnormal ploidy contributes to cystic kidney and aneurysm formation

Wissam A. AbouAlaiwi, Ph.D.[1*], Brian S. Muntean, B.Sc.[2*], Shobha Ratnam, M.D.[3], Bina Joe, Ph.D.[4], Lijun Liu, M.D.[5], Robert L. Booth, M.D.[6], Ingrid Rodriguez, D.O.[7], Britney S. Herbert, Ph.D.[8], Robert L. Bacallao, M.D.[9], Marcus Fruttiger, Ph.D.[10], Tak W. Mak, Ph.D.[11], Jing Zhou, M.D., Ph.D.[12], Surya M. Nauli, Ph.D.[1,2,3,4]

[*] These authors contribute equally.

[1]Department of Pharmacology, [2]Department of Medicinal and Biological Chemistry, [3]Department of Medicine, [4]Center for Hypertension and Personalized Medicine, [5]Department of Biochemistry and Cancer Biology, [6]Department of Pathology, The University of Toledo, Toledo, Ohio
[7]Department of Emergency and Intensive Care, ProMedica Sponsored Research, Toledo, Ohio
[8]Department of Medicine, [9]Department of Medical and Molecular Genetics, Indiana University School of Medicine, Indianapolis, Indiana
[10]UCL Institute of Ophthalmology, University College London, London, United Kingdom
[11]Ontario Cancer Institute, University Health Network, Toronto, ON, Canada
[12]Department of Medicine, Brigham and Women's Hospital, Boston, Massachusetts

Corresponding author:
Surya M. Nauli, Ph.D.
University of Toledo
Department of Pharmacology; MS 1015
Health Education building; Room 274
3000 Arlington Ave
Toledo, OH 43614

Phone: 419-383-1910
Fax: 419-383-1909
Email: Surya.Nauli@UToledo.Edu

SUPPLEMENTAL METHODS

Human tissues and cell lines

Signed and informed consent to collect disposed human tissues was obtained from the ADPKD (autosomal dominant polycystic kidney disease) and non-ADPKD patients. The protocols for tissue collection were approved by the Department for Human Research Protections of the Biomedical Institutional Review Board of The University of Toledo. Kidney tissues were collected from both ADPKD and non-ADPKD patients undergoing kidney transplant surgery. The non-cystic (male) and cystic (two males and one female) kidneys were obtained randomly from our hospital. Thus, these samples were not age-matched, but they are freshly collected within one hour after kidney removal from each patient. To ensure proper comparisons of human samples in our studies, we also used well-characterized human cell lines isolated from age- and sex-matched normal and PKD renal epithelia. Importantly, the PKD epithelial cells have been characterized to have abnormal cilia function. These cells also contain a marker of proximal nephron origin, which has previously been confirmed to have Q4004X mutation in *Pkd1* gene[1].

Genetic mouse models

All animal studies were approved by The University of Toledo animal care and use committee. We used both traditional and conditional transgenic mouse models in our present studies. We have previously obtained traditional transgenic *Pkd*-mouse models $Pkd2^{+/-}$ and $Tg737^{Orpk/Orpk}$ from Drs. Somlo[2] and Yoder[3], respectively. We used $survivin^{flox/flox}$ and $Pkd1^{flox/flox}$ conditional mouse models that were previously generated in our laboratories[4, 5]. To generate kidney-specific knockout, we used *Mx1Cre* mice previously confirmed with a *ROSA* model[5]. Briefly, one-week

old pups were injected intra-peritoneally with 62.5 μg of 50 μL polyinosinic:polycytidylic ribonuceic acid (pI:pC) every day for five consecutive days. In some cases, mice were subjected to renal injury at one-month old. Mice were sacrificed at either five-weeks or three-months of age, and their kidney morphologies were analyzed. To generate vascular-specific knockout, we used *PdgfβCre* mice previously confirmed with a *ROSA* model[6]. One-week old pups were injected intra-peritoneally with 250 μg of 50 μL tamoxifen every day for five consecutive days. In some cases, mice were subjected to vascular surgery at two-months old. Mice were sacrificed at three-months old, and their vascular morphologies were analyzed.

UUO and aneurysm inductions

Mouse health was confirmed before and after each surgical procedure. During the surgery, a mask connected to isoflurane regulator was placed over the nose and mouth of the mouse. 3-5% isoflurane was used to induce anesthetics followed by 1-3% isoflurane depending on the response to toe pinching and eye reflex. After shaving the hair around the incision site, skin was scrubbed with a betadine surgical scrub in circular motion from center out followed by 70% isopropyl alcohol. After the procedure was completed, the incision site was closed in a single layer using 4-0 silk suture. The skin was then closed using surgical staples (Clay Adams Autoclips). Mouse was monitored every 15 minutes until awake, followed by daily for 4 days post surgery. Only if the mouse was in pain, buprenorphine at 2.5/kg SQ twice a day was administered. Pain was determined by weight loss, lack of activity and failure to eat or drink. Penicillin G Procaine at 40,000 units/kg IM once a day was given if an infection was suspected. One sign of an infection would be discharge around the incision site.

To induce an experimental cystic model, unilateral ureteral obstruction (UUO) was generated by tying a 6-0 silk suture against a 28G needle in one-month old mice. After removal of the needle, a narrowing of total ureter diameter was achieved. The incision was sealed using a 4-0 silk suture followed by application of surgical staples to close the layer of skin. The mice were sacrificed one week later. To induce an experimental aneurysm model, sterile cotton gauze containing saline (control) or 0.25 M calcium chloride (aneurysm induction) was placed directly on the abdominal aorta for 10 minutes in two-month-old mice. Mice were euthanized at three-months old, at which time the heart and aorta were harvested, photographed, sectioned, and H&E stained to measure the diameter of the aneurysm lesions.

In both renal and vascular studies, we used respective UUO and $CaCl_2$ as models to facilitate and accelerate renal cyst and vascular aneurysm formation. These types of surgery models have been widely used to study kidney[7] and vascular[8] phenotypes. The advantages of such models include a rapid assessment of transgenic rodent models and provide a more precise location of injury, especially for mild aneurysm, which is very hard to spot within the vascular beds. In addition, these models are also characterized by an increased rate of cellular proliferation in kidney repair[7] and neovascularization[8]. This, in turn, will facilitate studying planar cell polarity, especially in non-PKD tissue. Consistent with this idea, it has been shown that cyst formation requires increased rates of cell proliferation[9], in which survivin is required. Although such operations may be less ideal in regard to mechanism and pathology comparison, we have thus collected data from zebrafish and PKD patients to further support our hypothesis. Of note is that increased cell proliferation is a major requirement of phenotypic development in human ADPKD kidney[10] and vascular endothelia[11].

Blood pressure measurement

Systolic and Diastolic blood pressure were monitored by non-invasive blood pressure system - tail cuff method with the aid of a computerized system (CODA system, Kent Scientific, Connecticut, USA). Measurements were performed at the baseline 3-times per week for 2 weeks after previous 3 days of training for each mouse. On each day of blood pressure measurement, 2 sets of 18 measurements were obtained including three measurements of training or acclimation. The measurements were averaged for each mouse with at least three mice for each genotype. All animals were tested by an investigator blinded to the genotypes of the animals. The data from the tail cuff method was also verified with limited studies with a more invasive, surgically implanted telemetry probe (data not shown).

Cell culture

Both primary cultures and cell lines were used in the present studies. The use and isolation of mouse primary tubular cells from distal collecting tubules have been described previously in detail[12]. For cell lines, we used previously generated endothelial cells from embryonic aortas. Various endothelial markers have been confirmed in these cells[13, 14]. More importantly, the mutant cell lines did not respond to fluid-shear stress, a characteristic of *PKD* cells with abnormal cilia function[1, 14]. All of these cells were subjected to cell sorting to obtain only those with normal chromosomal numbers. However, the rate of polyploidy or aneuploidy remains relatively constant in our mutant cells or human PKD cells. If we were to sort for polyploidy, they would not propagate further in culture. If we were to sort for diploidy, the polyploidy would appear within six passages, or even earlier. Thus, we believe that the “normal” PKD cells

will eventually become polyploidy or aneuploidy in a matter of time. In some cases, fluid-shear stress was applied to the surface of fully differentiated and confluent cells as previously described[13, 14].

Transfection study

For survivin-GFP experiments, human full-length survivin construct was inserted into pEGFPc1 (*Clontech, Inc.*) as previously described[11]. Cells were transiently transfected with the construct with Fugene 6, according to the manufacturer's instructions (*Roche Diagnostics, Inc.*). About 24 hours after transfection, cells expressing GFP were randomly selected for immunolocalization studies. For siRNA knockdown experiments, we purchased pre-designed commercially available siRNAs that have been previously characterized for PKC (*Santa Cruz Biotechnology, Inc.;* cat.#sc-29449), Akt (*Cell Signaling Inc.;* cat.#6211), aurora-A (*Ambion, Inc.*; cat.#s202070) and survivin (*Ambion, Inc.*; cat#s62463). All siRNAs were used at 10 μM and transfected into cells using Lipofectamine RNAiMAX following the manufacturer's protocol (*Invitrogen Inc.*).

Organ cultures

For *in vitro* analysis, we isolated kidneys from wild-type E15.5 mice. Individual kidney was then cultured on the transwell filter. DMEM culture medium containing 4 mM glutamine, 1X penicillin/streptomycin, 5 mg/mL insulin, 5 mg/mL transferrin and 5 ng/mL selenium was used in the absence or presence of 50 μM EM-1451 (*Erimos Pharmaceutics, Inc.*) or 100 μM VE-465 (*Merck, Inc.*). These concentrations were determined to be optimal conditions through dose-response studies (data not shown). The medium was supplied from underneath the transwell or the base of the filter to feed the kidney tissue. The medium was changed every day after

micrography of the kidneys with Nikon TE2000 microscope equipped with a color camera. Unless otherwise indicated, all culture media were obtained from *Fisher, Inc.*

Western analysis

Cultured cells were lysed with radioimmunoprecipitation assay (RIPA) buffer, and mouse kidneys and human kidney tissues were homogenized with RIPA buffer. Intracellular contents were collected by centrifugation at 100 *g* for 10 minutes. Total cell lysates were analyzed with a standard 8% SDS-PAGE. For protein isolation and Western analysis from zebrafish embryos, pooled embryos injected with control*MO, pkd2MO, pkd2MO* plus *survivin* mRNA, *survivin* mRNA alone, or *pkd2MO* plus VEGF were dechorionated and deyolked manually at 28 hpf stage and lysed with RIPA buffer containing protease inhibitor cocktail (*Roche*, Inc.). After determination of protein concentration (BCA assay kit, *Fisher Scientific*, Inc.), 50 μg of protein extract was loaded onto a 12% SDS-PAGE gels and transferred to nitrocellulose membranes.

The following primary antibodies were used for Western. pNF-κB (1:250), Akt (1:1,000), p-Akt (1:250), GAPDH (1:1,500), and cyclin-B1 (1:1,000) were obtained from *Cell Signaling, Inc.*; NF-κB (1:500) from *Santa Cruz Biotechnology Inc.*; aurora-A (1:1,000) from *BD Transduction, Inc.*; survivin (1:500) from *Novus Biologicals, LLC*; and actin (1:1,000) from *Sigma, Inc.*

Immunostaining study

Both actively dividing and fully differentiated cells were stained with various antibodies to study protein translocations and subcellular localizations. Longitudinal sections from mouse kidneys and aortas were also studied for cell division and mitotic spindle orientation. Briefly, cells and

tissues were fixed with 4% paraformaldehyde in 2% sucrose solution for 10 minutes at room temperature. After primary and secondary antibodies had been applied, samples were sandwiched on the microscope slide. They were observed with an inverted Nikon Ti-U microscope and analyzed three dimensionally with Metamorph 7.0. We have recently published a more detailed protocol and analysis of the longitudinal sections[15]. In some cases, a standard H&E and lectin staining was carried out. For zebrafish, whole-mount immunocytochemistry was performed using JB4 resin according to the manufacturer's instructions (Polyscience, Inc., Warrington, Philadelphia). Four-micron sections were cut by a Leica RM2255 microtome (Leica, Buffalo Grove, Illinois). Phenotypes were scored with a Nikon SMZ800 stereomicroscope equipped with a QImaging MicroPublisher 5.0 RTV color CCD camera operated by QCapture software.

Some kidney sections were immunostained with ZO-1, DBA (*dolichos biflorus* agglutinin) and WGA (wheat-germ agglutinin). ZO-1 recognizes tight junctions of renal epithelia; DBA is a lectin used as a marker for renal collecting ducts; WGA is a lectin found in all convoluted tubules as well as glomeruli in the kidney. We used these markers to generate contrast and indicate individual tubules in the renal phenotypic analyses. While ZO-1 was used in our planar cell polarity to highlight directions of tubular axes, DBA and WGA were used to indicate cyst or lumen areas. For the planar cell polarity analysis, we only counted dividing cells and measured the angle of nuclear division orientation relative to the orientation of the tubular axis as revealed by ZO-1 staining. For lumen/cyst areas, we measured lumen areas in DBA and/or WGA-positive cysts in both wild-type and *Mx1Cre:Survivin*$^{flox/flox}$ control and surgical kidney sections. Image acquisition and analysis were done with Metamorph 7.0.

Anti-survivin (1:500), aurora-A (1:1,000), NF-κB (1:500) antibodies were used for immunostaining. Antibodies purchased from *Vector Laboratories, Inc.* include rhodamine-labeled DBA (1:100), fluorescein-labeled WGA (1:100), rhodamine-conjugated phalloidin (1:500), and DAPI (1X). Other antibodies include pericentrin (1:1,000; *Covance, Inc.*), acetylated-α-tubulin (1:1,000; *Sigma, Inc.*), and ZO-1 (1:100; *ABCam, Inc*.).

Flow cytometry analysis

Cultured cells or freshly isolated cells from human, mouse and zebrafish were used in flow cytometry experiments. In some cases, cells were incubated with 30 μM 5-bromo-deoxyuridine (BrdU; *Sigma, Inc.*) for 15 minutes and rinsed with 1X PBS. The DNA was then denatured at 97 °C for 15 minutes and quickly chilled in an ice-water bath for 15 minutes. Anti-BrdU Alexa Fluor488 antibody was used at dilution of 1:100 (*Invitrogen, Corp.*). In apoptotic experiments, FITC conjugated annexin V antibody was used at dilution 1:100 (*Invitrogen, Inc*.). Propidium iodide at concentration of 20 μg/ml (PI; *Sigma, Inc.*) with or without counter-staining of phospho-Histone3B antibody (*Sigma, Inc.*) at dilution 1:100 was used in other experiments. Cells were analyzed with C6 Flow Cytometer (*Accuri Cytometers, Inc.*) using FL1, FL2 or FL3 detector to measure different fluorophore intensities.

Chromosomal analysis

Individual cells were isolated and incubated with 0.05 mg/ml colcemid solution for 30 minutes at 37 °C. The cells were incubated with 0.56% KCl solution for 45 minutes at 37 °C, followed by fixing with 3:1 (v/v) methanol:acetic acid. Individual cells were dropped onto a pre-cleaned

glass slide and counter stained with DAPI. After sequential digestion with RNase and pepsin, the chromosomal DNA on the slide was denatured in 70% formamide and then hybridized with a cocktail of mouse or human SKY paint probes tagged with various nucleotide analogues according to the procedure recommended by *Applied Spectral Imaging*, Inc. (ASI; Vista, CA). The images from combinations of five different fluorophores were developed and analyzed. Rhodamine, Texas-Red, Cy5, FITC and Cy5.5 were captured with a spectral cube and interferometer module installed on an Olympus microscope. Spectral-Karyotypes were carried out using SKY View software (Version 1.62).

For zebrafish chromosome spreading, eggs were collected at the two-cell stage and injected with control*MO*, *pkd2MO*, *pkd2MO* plus *survivin* mRNA, *survivin* mRNA alone, or *pkd2MO* plus VEGF. Because these cells were actively dividing and developing into embryos at this period, three hours incubation was sufficient for the morpholinos, mRNA or VEGF to take effect. These three-hours postfertilization (hpf) eggs contained about 1,000 cells. Next, 0.02% colchicine was added for an additional four hours before the choriones were removed with protease solution. De-chorionated embryos were then incubated in 0.56% KCl solution for 40 minutes and fixed with 3:1 (v/v) methanol:acetic acid solution for 20 minutes. Chromosomes were spread on the slide for analysis after DAPI staining. Because zebrafish chromosome-specific probes for chromosomal spectral karyotype analysis are not available, we characterized individual chromosomes based on the ideogram derived from the replication banding of *Danio rerio*[16].

Live-imaging study

Primary renal epithelial cells or vascular endothelial cells were transfected with or without *Survivin* siRNA. Cells were then incubated with membrane-permeable and DNA-specific dye, Hoechst for 20 minutes. One Randomly selected cells from each group were studied and recorded with a Nikon TE2000 microscope equipped with an environmental chamber. Hoechst fluorescence and high-resolution differential interference contrast images were captured every 2-5 minutes at exposure time of 500 and 100 milliseconds, respectively. For better focusing, the microscope was equipped with XY-axis motorized flat top inverted stage, automatic focusing RFA Z-axis drive, and custom-designed vibration isolation platform. For a better-controlled environment, the body of the microscope was enclosed inside a custom-built chamber to control CO_2, humidity, heat and light.

Zebrafish study

Wild-type (wt) zebrafish AB strains were maintained according to standard protocols used to maintain and raise wt strains and embryos. Embryos were cultured at 28.5°C in 0.0045% phenylthiourea in a Danieau buffer to inhibit pigmentation. Zebrafish embryos were microinjected at the 1-2 cell stage with 1 mM antisense morpholino (*MO*) oligonucleotides obtained from GeneTools (Philomath, OR). A volume of 1 nL of *pkd2MO* (translational blocking *MO*) that targets against the 5'UTR of *pkd2* (*pkd2MO:* 5′-AGG ACG AAC GCG ACT GGA GCT CAT C-3′) was injected using a Narishige IM-9B microinjector (East Meadow, New York) controlled by a Narishige NAI-2N micromanipulator (East Meadow, New York) to deliver 9.0 ng into the embryo. As a control, zebrafish embryos were injected with 1-2 nL of *controlMO* (5′-CCT CTT ACC TCA GTT ACA ATT TAT A-3′) to deliver 6-12 ng into the embryo. Note

that both of these *MO*s have been previously utilized[17-19]. Un-injected control embryos were also used to verify the studies (data not shown). For rescue experiments, full-length human survivin gene (without GFP) was cloned in the survivin vector as described previously[11]. After linearization, the plasmids were transcribed *in vitro* with T7 RNA polymerase using the mMESSAGE mMACHINE kit from *Ambion* (Austin, TX, USA). 100 pg of purified *survivin* mRNA were either co-injected with *pkd2* morpholinos or alone into the 1-2 cell-stage embryos. In another case, 2.5 ng vascular endothelial growth factor (VEGF) was co-injected with *pkd2* morpholinos.

SUPPLEMENTAL FIGURE & FIGURE LEGENDS

Supplemental Figure 1a

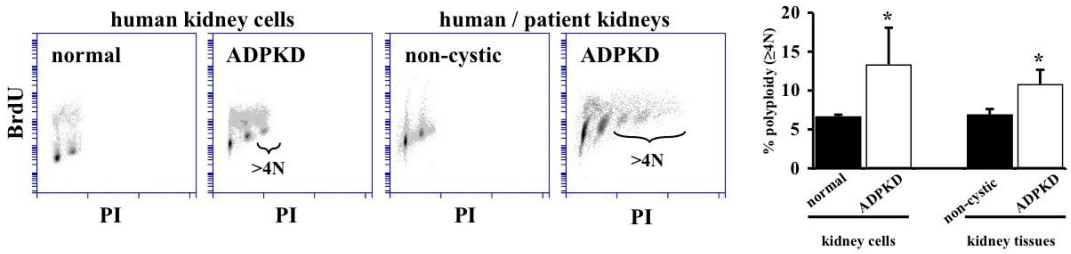

Supplemental Figure 1b

normal kidney cell (46, XY)

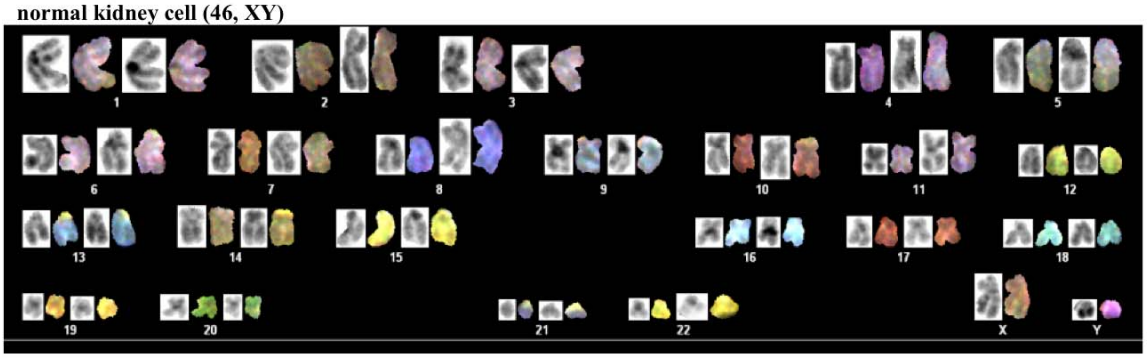

ADPKD kidney cell (45, XY, -4)

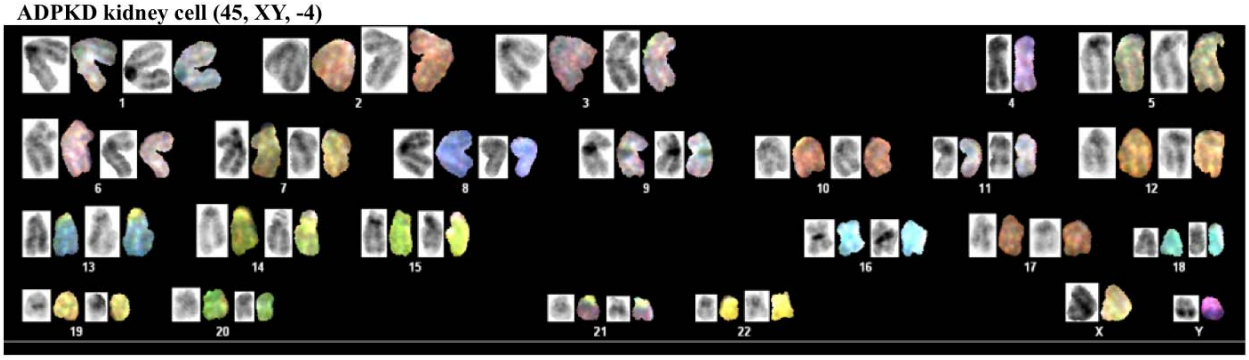

kidney cell line	normal	tetraploidy	aneuploidy	count (N)	% abnormal
non-ADPKD	9	0	2	11	18
ADPKD	20	1	6	27	26

Supplemental Figure 1c

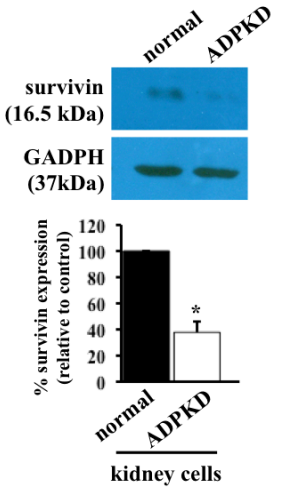

Supplemental Figure 1d

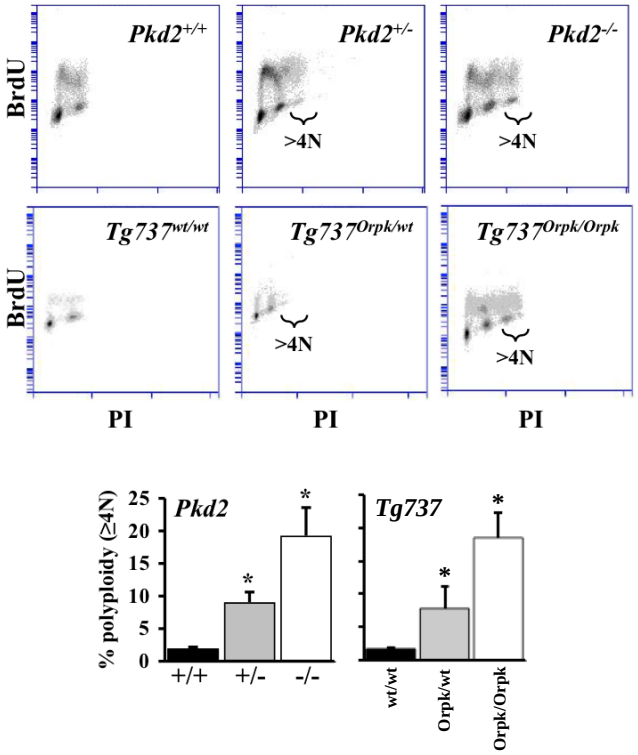

Supplemental Figure 1e

Pkd2$^{+/+}$ (40, XX)

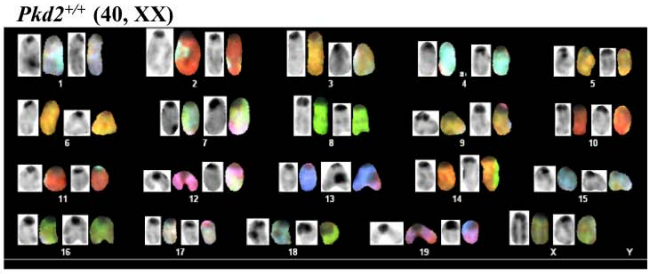

Pkd2$^{-/-}$ (80, XXYY)

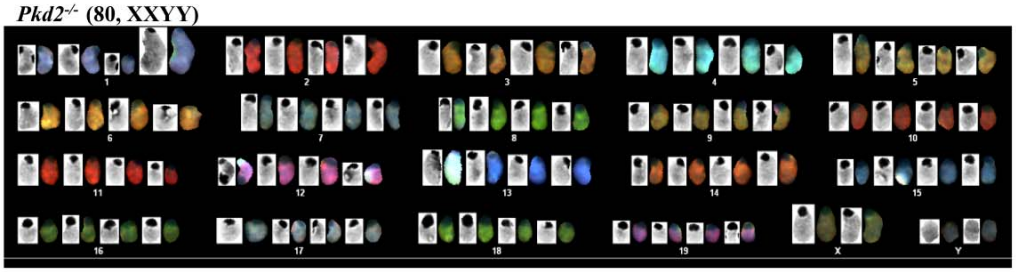

Pkd2$^{+/-}$ (160, XXXXXXXX)

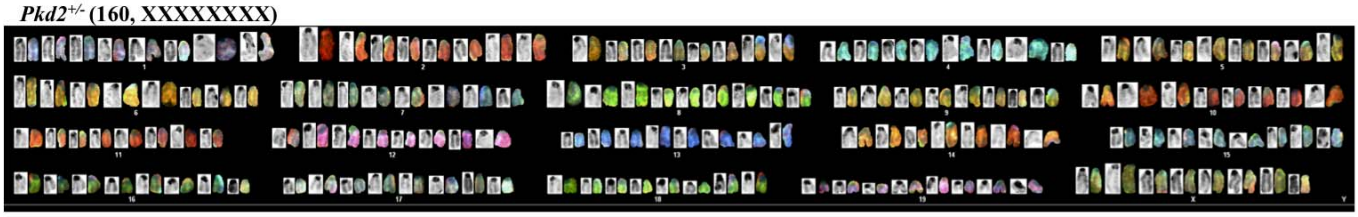

samples		normal	tetraploidy	aneuploidy	count (N)	% abnormal
mouse kidneys	*Pkd2*$^{+/+}$	19	2	0	21	9
	Pkd2$^{+/-}$	8	12	1	21	62
	Pkd2$^{-/-}$	11	13	1	25	56

Supplemental Figure 1f

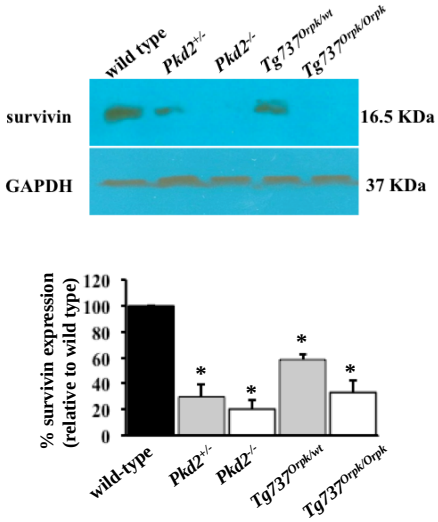

Supplemental Figure 1. Human ADPKD and mouse *Pkd* kidney epithelia are characterized by abnormal ploidy level and survivin down-regulation.

(**a**) Previously characterized human cell lines from normal and ADPKD kidneys were analyzed for their cellular divisions with flow cytometry by BrdU and PI staining. We first pre-sorted and collected only diploid cells (2N). Over the next 5-10 passages, we observed that compared to non-cystic cells, ADPKD-derived cells have a greater chance of producing genetic instability in their chromosomal composition. Bar graph shows that epithelia from both *ADPKD* kidney cells contain a greater polyploidy with DNA content of >4N compared to non-ADPKD or normal ones. (**b**) Further karyotype analysis of individual cells confirms the presence of abnormal genomic compositions (aneuploidy or polyploidy) in ADPKD cells. (**c**) Human cell lines were also used to confirm survivin expression, and GADPH was used as loading control. Bar graph shows relative survivin expression levels. (**d**) Representative BrdU and PI labeling profiles reveal an increase in cell polyploidy in kidneys from both heterozygous (*Pkd2*$^{+/-}$ or *Tg737*$^{Orpk/wt}$) and homozygous (*Pkd2*$^{-/-}$ or *Tg737*$^{Orpk/Orpk}$) mice compared to the corresponding wild-type (*Pkd2*$^{+/+}$ or *Tg737*$^{wt/wt}$). Bar graph shows that epithelia from both *Pkd2* and *Tg737* kidneys, compared to their wild-type kidneys, significantly contain greater polyploidy with DNA content of >4N. (**e**) Karyotyping was carried out in freshly isolated cells from *Pkd2*$^{+/+}$, *Pkd2*$^{+/-}$ and *Pkd2*$^{-/-}$ kidneys to visualize individual chromosomes. A simple chromosome count indicates the presence of polyploidy cells in both *Pkd2*$^{+/-}$ and *Pkd2*$^{-/-}$ kidneys. Further characterization of individual chromosomes with fluorescence probes indicates the polyploid and aneuploid nature of *Pkd2*$^{+/-}$ and *Pkd2*$^{-/-}$ kidneys. (**f**) Embryonic kidneys were pooled and analyzed for survivin expression, and GAPDH was used as loading control. Bar graph shows relative survivin

expression levels. For flow cytometry and Western experiments, N≥4 for independent kidney isolations for each genotype (analyzed with ANOVA test followed by Dunn's Multiple Comparison posttest analysis) and each human cell line (analyzed with paired Student *t*-test).

Supplemental Figure 2a

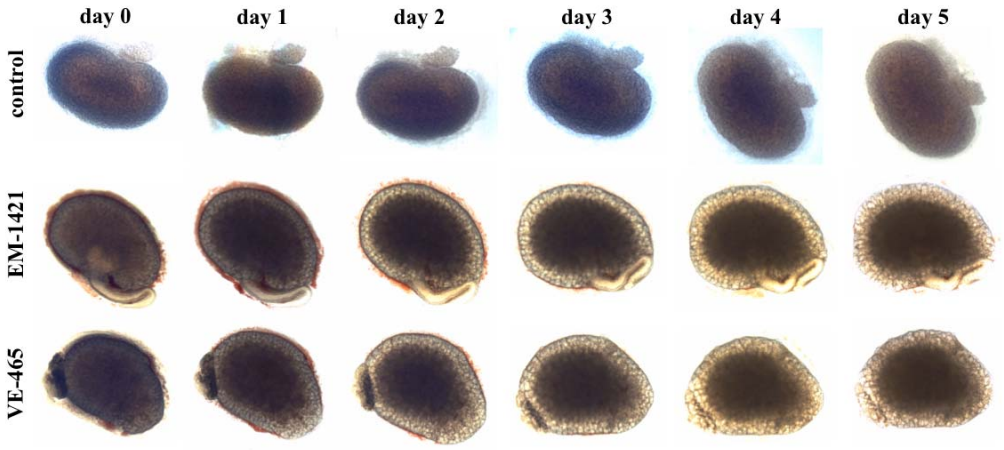

Supplemental Figure 2b

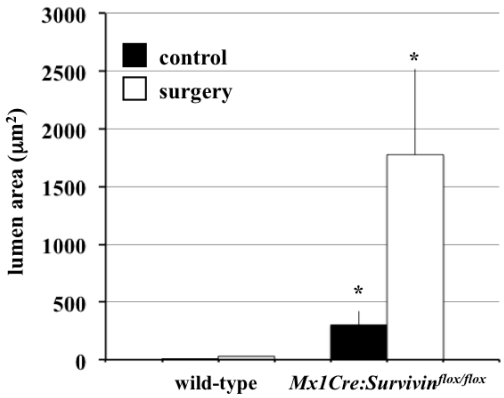

Supplemental Figure 2c

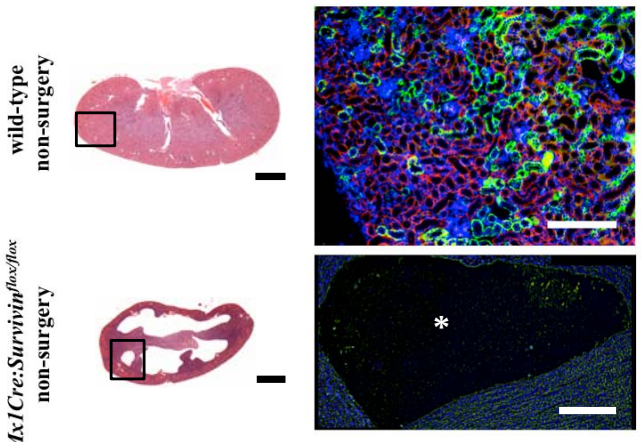

Supplemental Figure 2. Survivin downregulation is sufficient to induce cystic kidney formation.

(**a**) Embryonic kidneys from E15.5 of the same litter were isolated and cultured on transwell filters. After the first micrographs were taken at day 0, cultures were then treated with vehicle as control, 50 μM EM-1451 or 100 μM VE-465 to induce abnormal cell division by inhibiting survivin or aurora-A kinase, respectively. Kidney cultures were micrographed daily for a total of six days. Cyst-like phenotype was apparent as early as day 2. (**b**) Bar graph shows quantitation of lumen sizes (cyst areas) in wild-type and *Survivin* knockout kidneys. A total of 30-53 lumen areas were measured from three randomly selected kidneys in each group. (**c**) Paralleled kidney sections were obtained from three-months old mice for H&E and fluorescence analyses. Box in the H&E kidney corresponds to an approximate area for further fluorescence study. White asterisk indicates renal cyst. N≥3 for kidney analysis in each group and genotype (analyzed with ANOVA test followed by Dunn's Multiple Comparison posttest analysis). White bar=200 μm; black bar=1 mm.

Supplemental Figure 3a

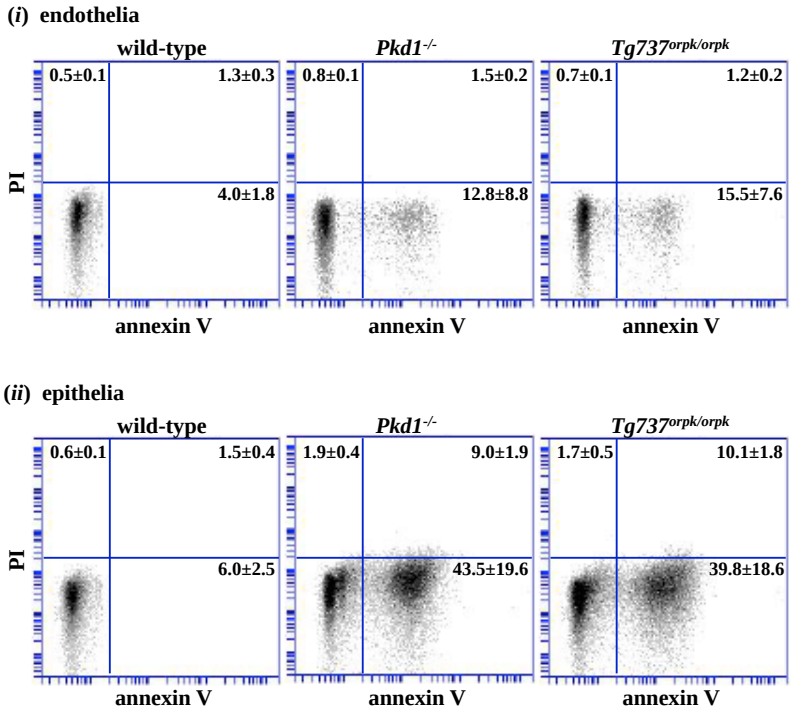

Supplemental Figure 3b

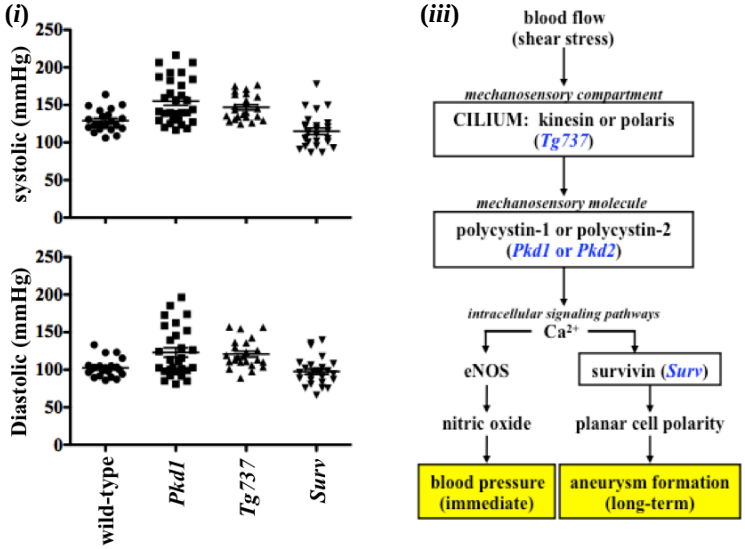

(*ii*)

	systolic (mmHg)	diastolic (mmHg)	N
wild-type	128±9	102±7	3
Pdgfbcre:Pkd1$^{flox/flox}$	150±19*	120±21*	4
Tie2Cre:Tg737$^{flox/flox}$	147±10*	120±11*	3
Pdgfβcre:Surv$^{flox/flox}$	114±13	99±13	3
** significant different from wild-type control*			

Supplemental Figure 3. Apoptosis and blood pressure measurements.

(**a**) Compared to the corresponding control wild-type cells, apoptosis is significantly greater in vascular endothelial (***i***) and renal epithelial (***ii***) of *Pkd1* and *Tg737* mutant cells. Annexin V is used as an early apoptotic marker, and propidium iodide (PI) is used as a necrotic marker. (**b**) *Pdgfβcre:Survivin*$^{flox/flox}$ mice do not have elevated systolic or diastolic blood pressure. Blood pressure was measured in wild-type and conditional *Pkd1*, *Tg737*, and *Survivin* (*Sur*) mice for a 2-week period (***i***). The averaged measurements of blood pressure during this 2-week period were tabulated (***ii***). A working model is presented showing the roles of primary cilia in blood pressure and aneurysm formation (***iii***).

Supplemental Figure 4a

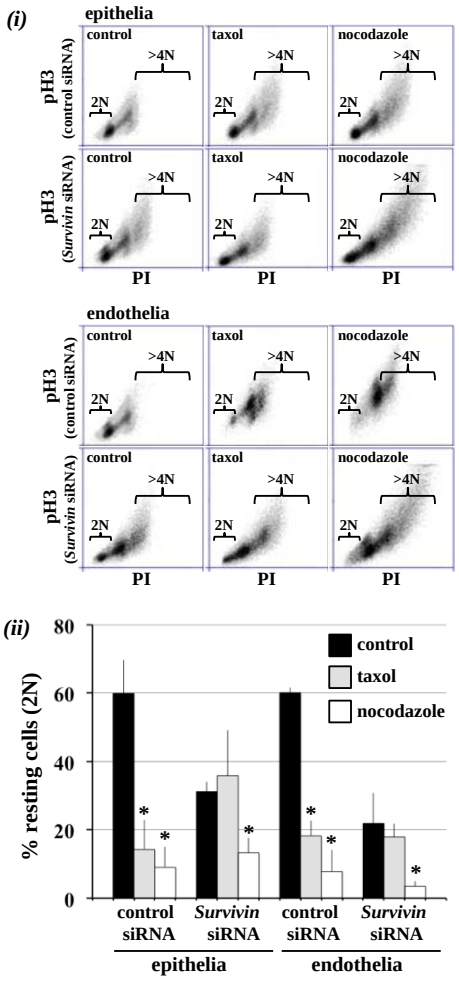

Supplemental Figure 4b

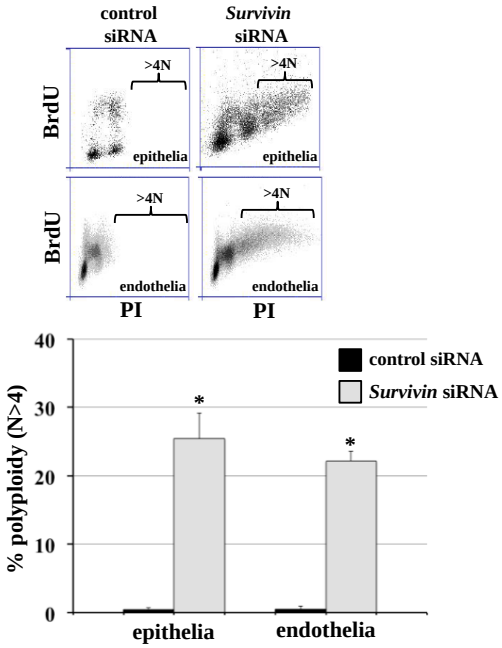

Supplemental Figure 4. Survivin down-regulation is associated with abnormal cytokinesis in primary cells of renal epithelia and vascular endothelial cells.

(**a-*i***) Mitotic-stress test indicates abnormal cytokinesis associated with knockdown of a chromosomal passenger protein (survivin). Cell-cycle arrest was induced with taxol or nocodazole to stabilize or depolymerize mitotic spindles, respectively. Those cells with abnormal chromosomal passenger protein expression were not inhibited in cell arrest-induced by taxol. Phospho-histone3b (pH3) and PI were used to differentiate those cells that were not arrested by taxol. (**a-*ii***) Mitotic stress was measured by analyzing changes in resting cells (2N), which are PI- and pH3-negative, from the total cell population. The test would thus examine if survivin down-regulation is responsible for a cell escaping cell-cycle arrest in the presence of taxol. The results from the mitotic-stress test indeed indicate that knockdown of survivin expression was characterized by abnormal cytokinesis. Although most normal cells could be arrested by nocodazole (microtubule depolymerizer) and taxol (microtubule stabilizer), survivin knockdown cells could only be arrested by nocodazole. This is consistent with previous reports showing that cells with abnormal chromosomal passenger complex, such as survivin, would not be arrested by taxol. (**b**) To validate that *Survivin* knockdown would induce abnormal cytokinesis leading to polyploidy, cell-cycle profile was analyzed with PI and BrdU to study cellular proliferation in epithelial and endothelial cells. Bar graph shows that compared to corresponding control groups, survivin knockdown-epithelia and endothelia contain significantly more polyploidy with DNA content of >4N. Bar=50 μm. $N \geq 3$ for each group and treatment (analyzed with ANOVA test followed by Dunn's Multiple Comparison posttest analysis).

Supplemental Figure 5a

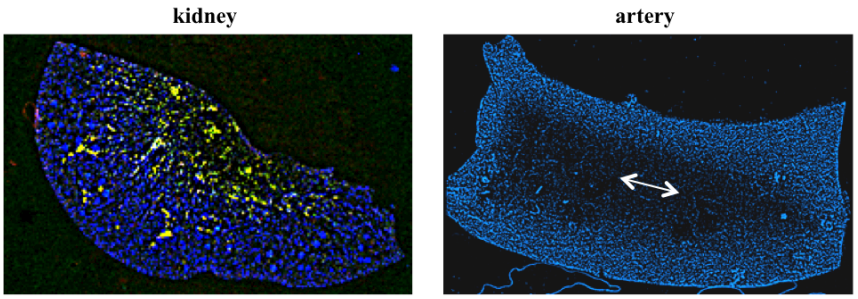

Supplemental Figure 5b

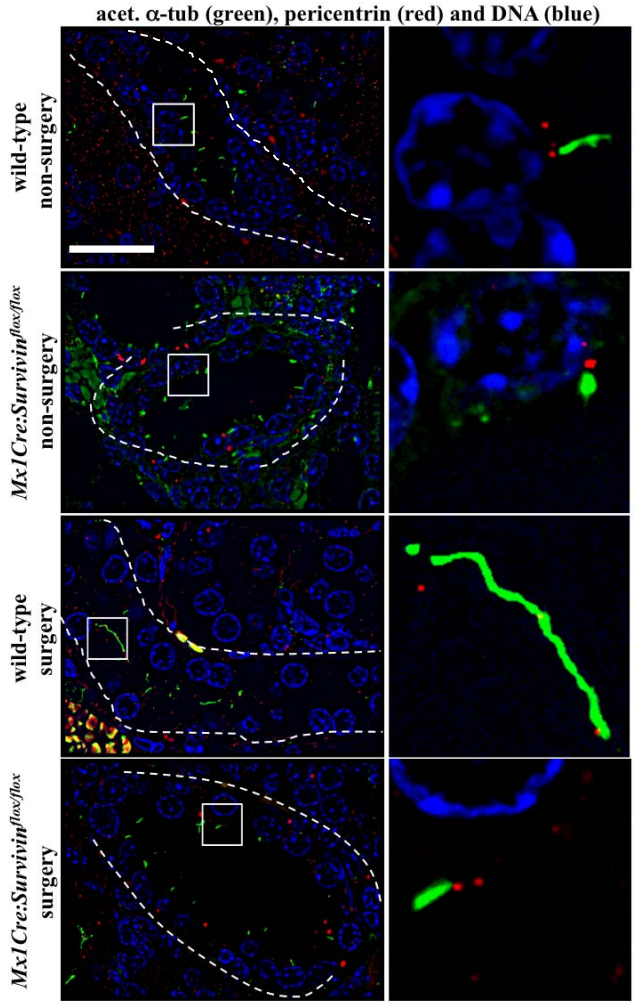

Supplemental Figure 5c

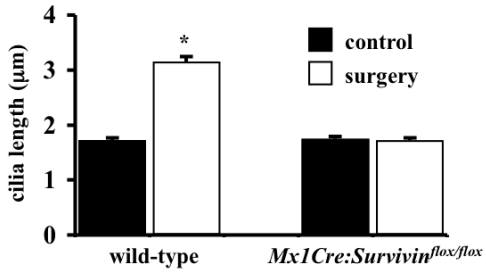

Supplemental Figure 5d

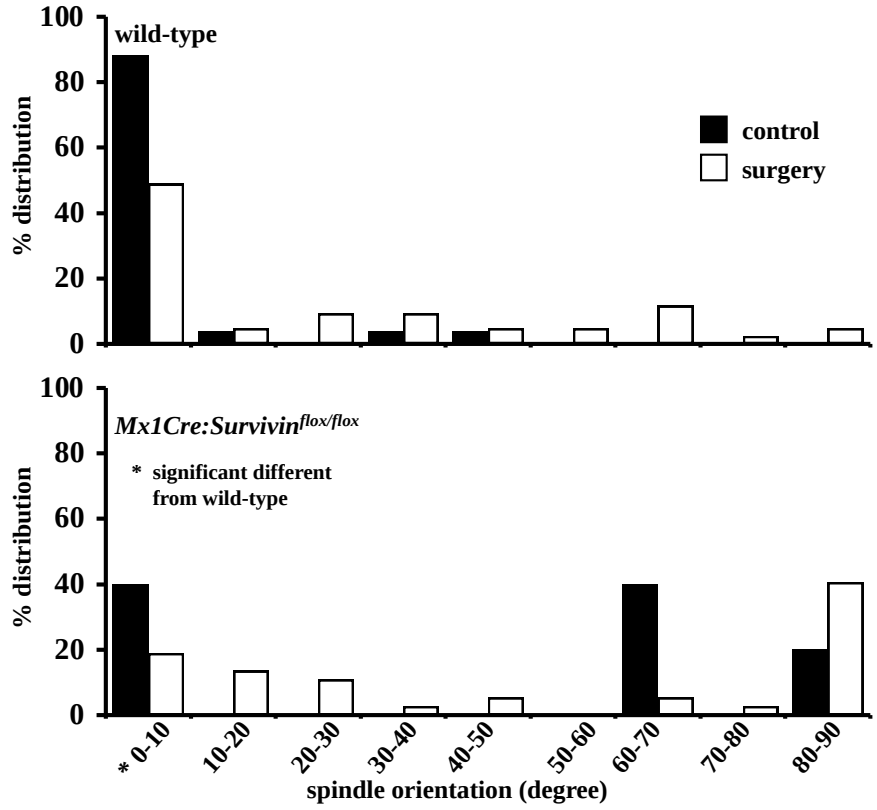

Supplemental Figure 5. Abnormal cellular division orientation is associated with renal cystic and vascular aneurysm phenotypes.

(**a**) Mouse kidney and artery longitudinal sections stained with acetylated-α-tubulin (green), pericentrin (red), and DAPI (blue) were used to examine cell division orientation. (**b**) Longitudinal kidney tubular sections from wild-type and *Mx1Cre:survivin*$^{flox/flox}$ mice with or without UUO surgery were used to study structural length of primary cilia. Longer cilia were observed in tubular sections of wild-type UUO kidneys. White box indicates the enlargement of the region within the kidney lumen. (**c**) The length of cilia in wild-type kidney tubules was significantly increased following UUO surgery but not in *Mx1Cre:survivin*$^{flox/flox}$ mice. (**d**) The frequency distribution of cell-division orientation angle (degrees) was tabulated in control and surgical kidneys in both wild-type and *Mx1Cre:survivin*$^{flox/flox}$ mice. Angles of cell-division orientation in *Mx1Cre:survivin*$^{flox/flox}$ mice show a shift towards the higher angle groups in both control and surgical kidneys. N≥3 for each group and genotype. N≥100 for distribution of spindle orientation angle for each genotype and each treatment. N≥1,600 for cilia length measurement. Bar=40 μm.

Supplemental Figure 6a

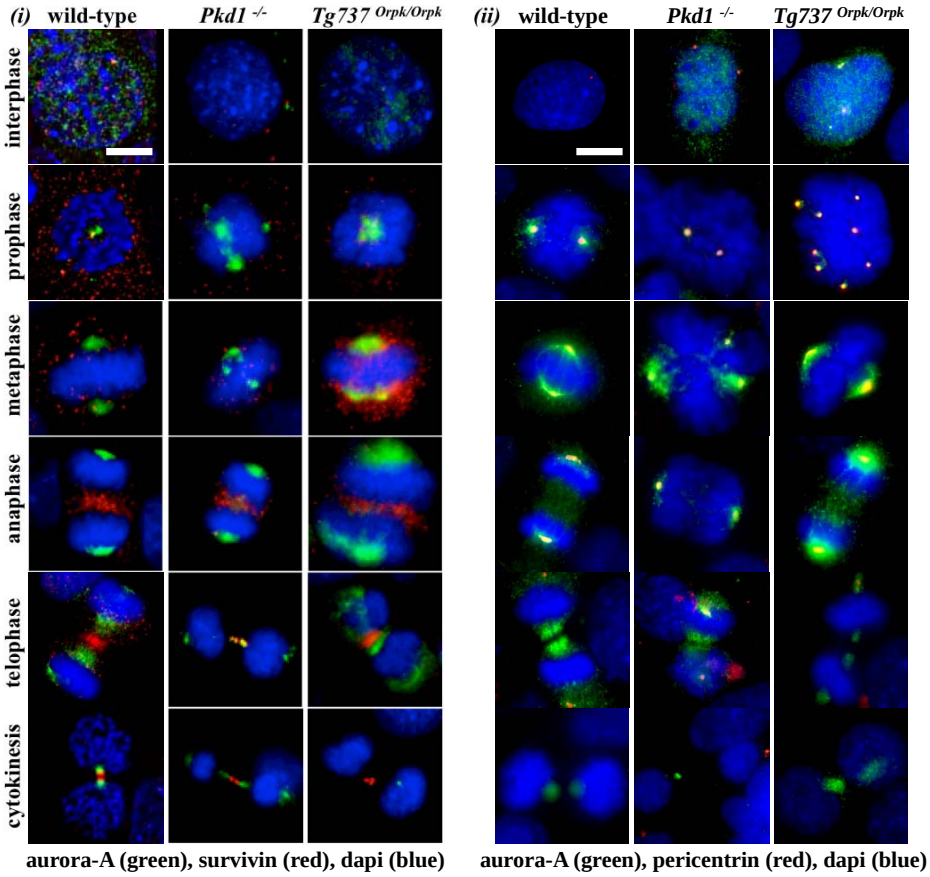

Supplemental Figure 6b

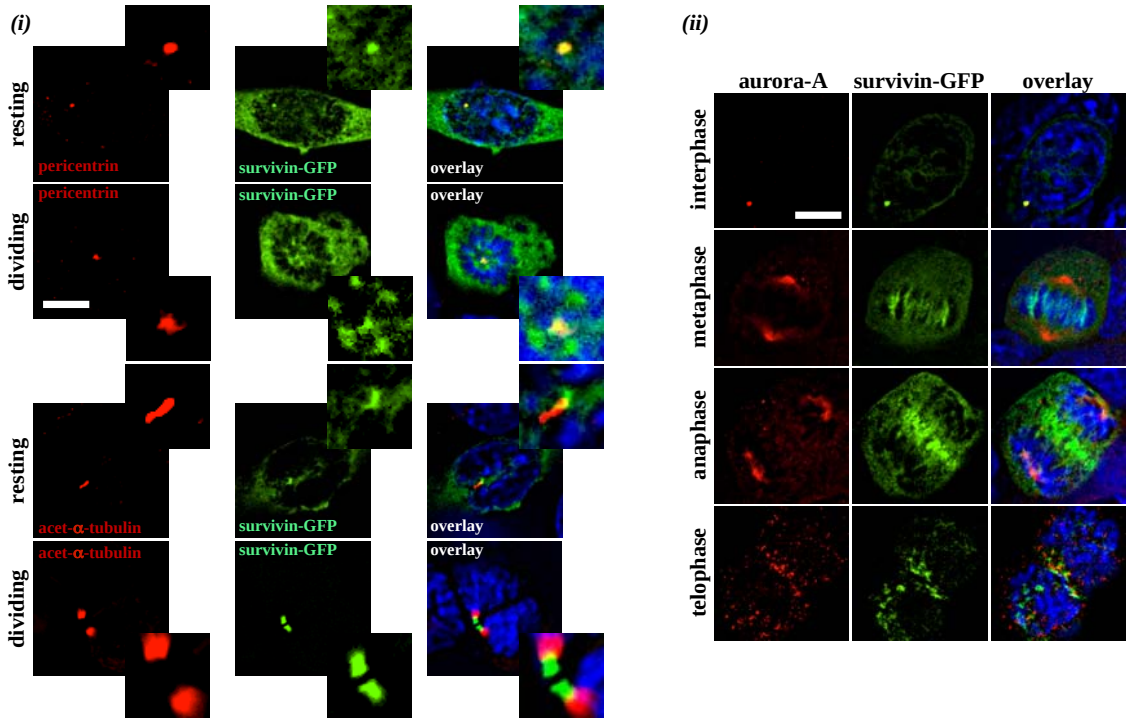

Supplemental Figure 6. Confirmations of survivin antibody and survivin/aurora-A localization. (**a**) Cells were stained with aurora-A (green) and survivin (***i***; red) or pericentrin (***ii***; red). To study subcellular localization of aurora-A and survivin, images were captured at different cell-cycle stages of interphase, prophase, metaphase, anaphase, telophase and cytokinesis. Aurora-A and survivin are localized to the centriole in interphase, the centrosome in prophase and the mid-body during telophase and cytokinesis. (**b**) Cells were transfected with survivin-GFP (green) and stained with pericentrin/acetylated-α-tubulin (***i***; red) or aurora-A (***ii***; red). Subcellular localizations of survivin/aurora-A were studied in resting and dividing cells. Insert shows area of enlargement for survivin/pericentrin/acetylated-α-tubulin localization. Bar=10 μm.

Supplemental Figure 7a

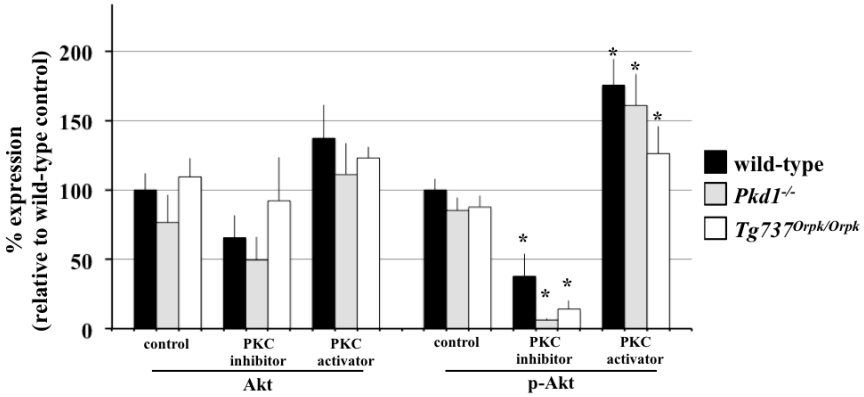

Supplemental Figure 7b

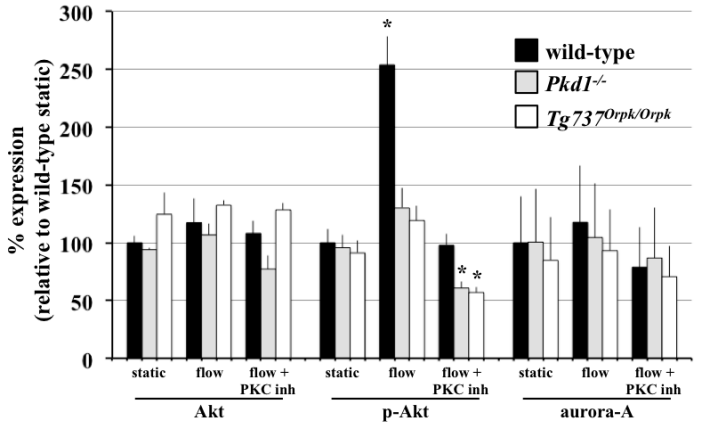

Supplemental Figure 7c

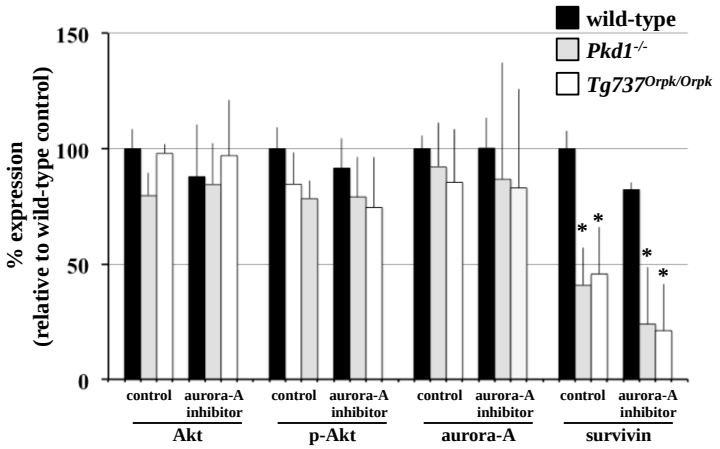

Supplemental Figure 7d

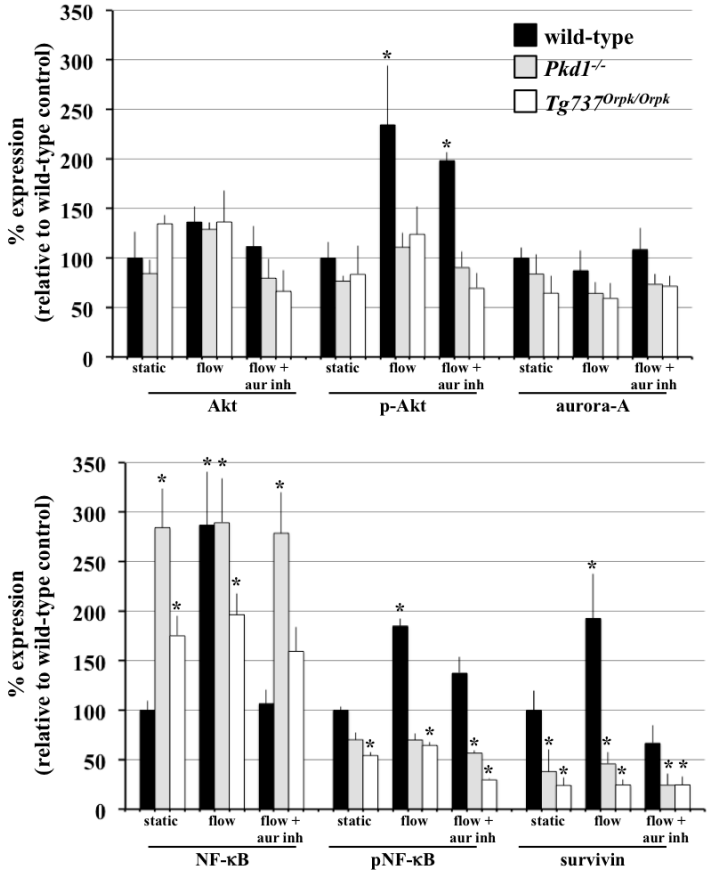

Supplemental Figure 7e

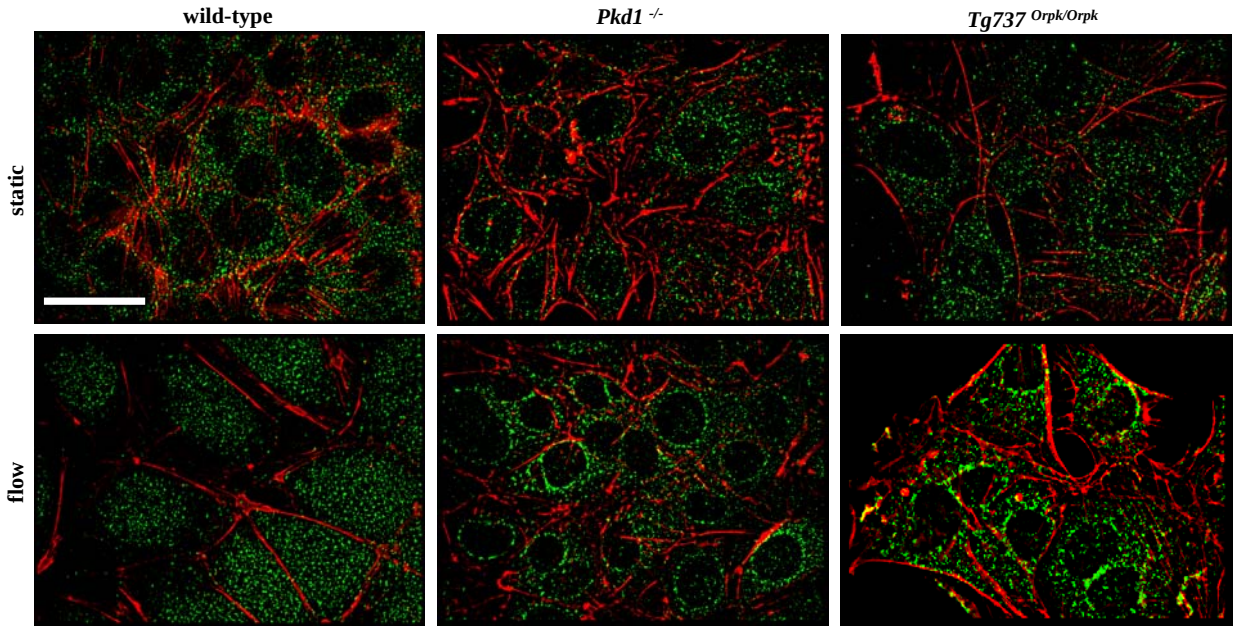

NF-κb (green), actin (red)

Supplemental Figure 7f

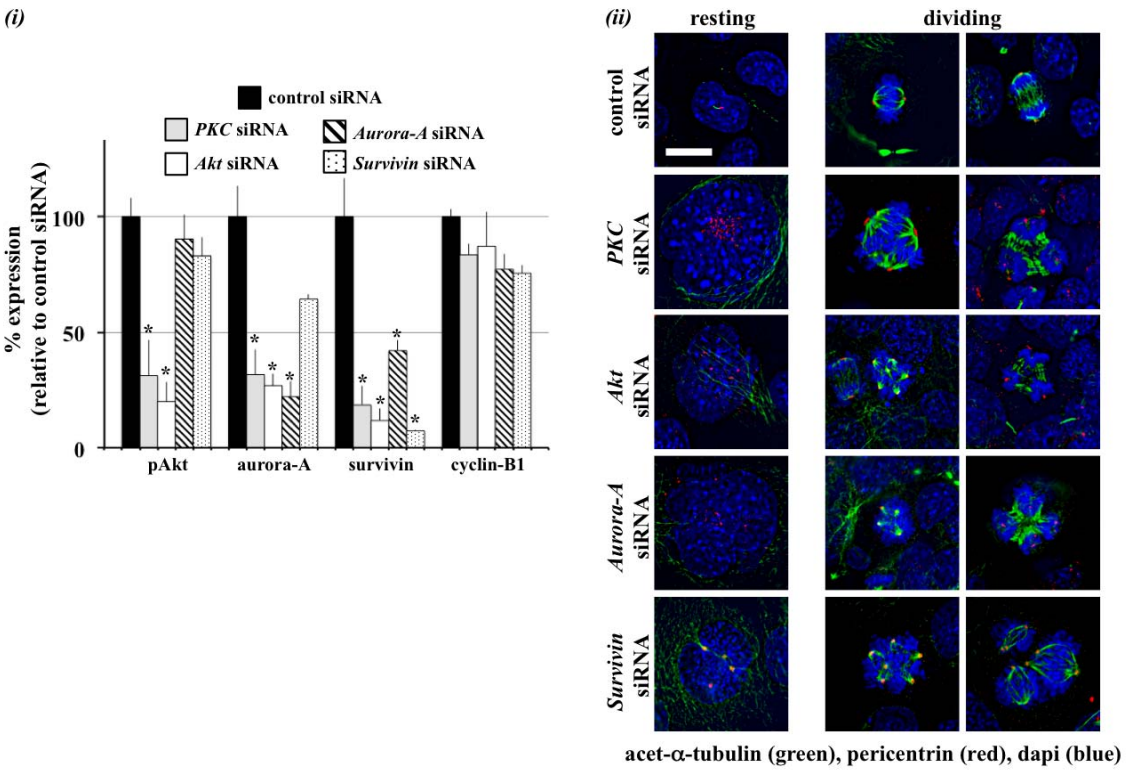

Supplemental Figure 7g

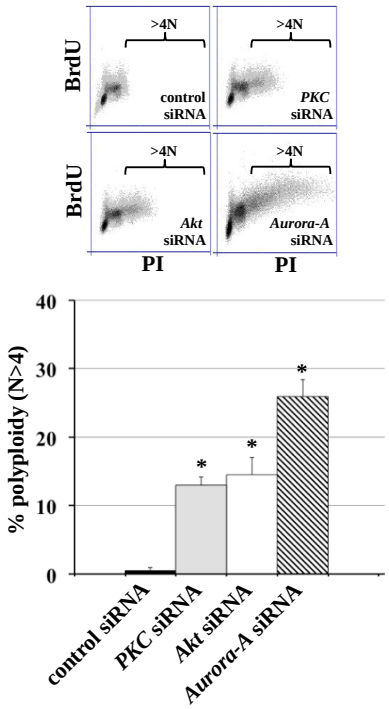

Supplemental Figure 7. PKC/Akt/NF-κB signaling pathway regulates flow-induced survivin expression and cell division.

(**a**) After wild-type and cilia mutant (*Pkd1*$^{-/-}$ and *Tg737*$^{Orpk/Orpk}$) cells were treated with PKC inhibitor or activator, both Akt and p-Akt were analyzed. When treated with PKC inhibitor, all cell lines showed down-regulation of p-Akt, while PKC activator treatment showed an increase in p-Akt compared to non-treated control cells. (**b**) The effect of fluid-flow on Akt and aurora-A expression was analyzed in the presence or absence of PKC inhibitor. When subjected to fluid-shear, p-Akt expression was up-regulated only in wild-type cells. While p-Akt expression returned to basal levels following treatment with PKC inhibitor and fluid-shear stress in wild-type cells, it stayed repressed in mutant cells. (**c**) Treatment with aurora-A inhibitor resulted in a decrease in p-Akt, aurora-A and survivin expression; however, these decreases were not significant from the control, non-treated group. (**d**) While total Akt level was not changed, fluid-shear stress significantly induced expression of p-Akt in wild-type but not in mutant cells. Aurora-A expression was increased following fluid-shear stress in wild-type cells; however, this increase was not significant from control. Both NF-κB and pNF-κB expressions were increased following fluid-shear stress only in wild-type cells, while mutant cells maintained a high basal level of NF-κB compared to static wild-type cells. Survivin expression was increased following shear-stress in wild-type cells. (**e**) NF-κB nuclear translocation was confirmed with immunostaining study. Cells were stained with NF-κB p65 (green), actin (red) to examine subcellular localization of NF-κB before and after fluid flow. In contrast to mutant cells, wild-type cells show NF-κB translocation from cytoplasm to nucleus when subjected to fluid-shear stress. (**f-*i***) Western blot analyses were conducted to confirm the signaling mechanism involving survivin expression by siRNA-mediated knockdown of PKC, Akt, aurora A, or survivin. (**f-*ii***)

To further confirm the involvement of these signaling molecules in centrosome number and cell division abnormality, immunofluorescence analysis was performed using acetylated-α-tubulin and pericentrin. (**g**) Flow cytometry was done to analyze ploidy level in PKC, Akt or aurora-A knockdown cells. Bar=40 μm. N≥3 for each group and treatment. All Western blot analyses were done by comparing treatment groups to their corresponding wild-type control, non-treated groups. Data analysis was performed with ANOVA test followed by Dunn's Multiple Comparison posttest analysis

Supplemental Figure 8a

overall phenotypic observations

28 hpf n/total (%)	curly tail	renal cyst
control *MO*	0/61 (0)	N/A
pkd2 MO	55/70 (79)	N/A
pkd2 + *survivin* mRNA	36/95 (38)	N/A
survivin mRNA	0/53 (0)	N/A
pkd2 + VEGF	22/67 (33)	N/A
48 hpf n/total (%)	**curly tail**	**renal cyst**
control *MO*	0/45 (0)	0/25 (0)
pkd2 MO	36/46 (78)	24/29 (83)
pkd2 + *survivin* mRNA	24/63 (38)	10/26 (38)
survivin mRNA	0/42 (0)	0/25 (0)
pkd2 + VEGF	30/67 (45)	14/28 (50)
72 hpf n/total (%)	**curly tail**	**renal cyst**
control *MO*	0/45 (0)	0/27 (0)
pkd2 MO	36/46 (78)	23/26 (88)
pkd2 + *survivin* mRNA	28/61 (46)	19/28 (68)
survivin mRNA	0/42 (0)	0/21 (0)
pkd2 + VEGF	45/67 (67)	19/26 (73)

Supplemental Figure 8b

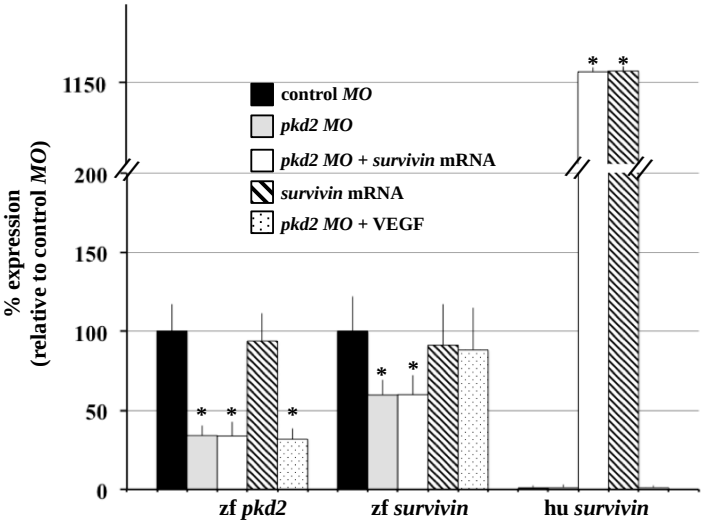

Supplemental Figure 8c

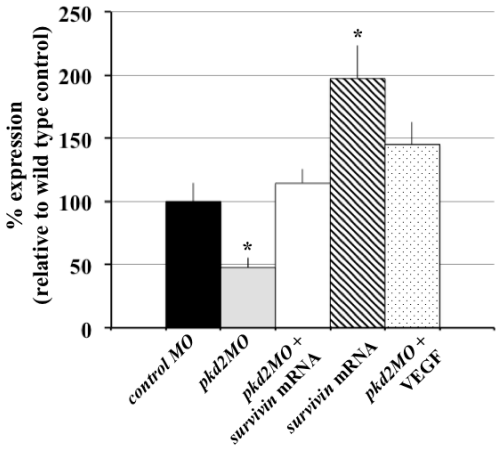

Supplemental Figure 8d

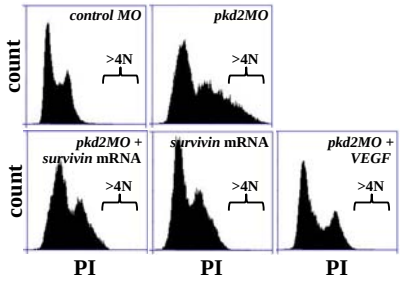

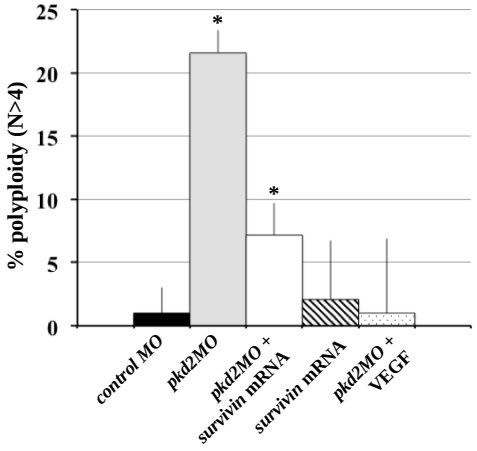

Supplemental Figure 8. Survivin overexpression rescued PKD phenotypes in zebrafish.

(**a**) An overall phenotypic was tabulated for wild-type, curly tail and renal cyst phenotypes in zebrafish injected with either control *MO*, *pkd2* MO, *pkd2 MO* plus *survivin* mRNA, *survivin* mRNA alone, or *pkd2 MO* plus VEGF. (**b**) RT-PCR was performed to examine zebrafish (zf) and human (hu) transcript levels for *survivin* and to confirm *pkd2* knockdown. Human survivin was introduced through mRNA injection. α-tubulin was used as a loading control. (**c**) Expression levels of survivin were analyzed in all the groups, in which zebrafish and human survivin can be recognized by the same antibody. (**d**) Polyploidy level was also validated and quantified with flow cytometry by isolating cells from each group of zebrafish. $N \geq 4$ for each group and treatment. All Western blot and RT-PCR analyses were done by comparing injected groups to the control *MO* group. Data analysis was performed with ANOVA test followed by Dunn's Multiple Comparison posttest analysis

SUPPLEMENTAL REFERENCES

1. Xu C, Shmukler BE, Nishimura K, Kaczmarek E, Rossetti S, Harris PC, Wandinger-Ness A, Bacallao RL, Alper SL. Attenuated, flow-induced atp release contributes to absence of flow-sensitive, purinergic cai2+ signaling in human adpkd cyst epithelial cells. *American journal of physiology*. 2009;296:F1464-1476
2. Wu G, Markowitz GS, Li L, D'Agati VD, Factor SM, Geng L, Tibara S, Tuchman J, Cai Y, Park JH, van Adelsberg J, Hou H, Jr., Kucherlapati R, Edelmann W, Somlo S. Cardiac defects and renal failure in mice with targeted mutations in pkd2. *Nature genetics*. 2000;24:75-78
3. Moyer JH, Lee-Tischler MJ, Kwon HY, Schrick JJ, Avner ED, Sweeney WE, Godfrey VL, Cacheiro NL, Wilkinson JE, Woychik RP. Candidate gene associated with a mutation causing recessive polycystic kidney disease in mice. *Science (New York, N.Y.* 1994;264:1329-1333
4. Okada H, Bakal C, Shahinian A, Elia A, Wakeham A, Suh WK, Duncan GS, Ciofani M, Rottapel R, Zuniga-Pflucker JC, Mak TW. Survivin loss in thymocytes triggers p53-mediated growth arrest and p53-independent cell death. *The Journal of experimental medicine*. 2004;199:399-410
5. Takakura A, Contrino L, Beck AW, Zhou J. Pkd1 inactivation induced in adulthood produces focal cystic disease. *J Am Soc Nephrol*. 2008;19:2351-2363
6. Claxton S, Kostourou V, Jadeja S, Chambon P, Hodivala-Dilke K, Fruttiger M. Efficient, inducible cre-recombinase activation in vascular endothelium. *Genesis*. 2008;46:74-80
7. Yang L, Besschetnova TY, Brooks CR, Shah JV, Bonventre JV. Epithelial cell cycle arrest in g2/m mediates kidney fibrosis after injury. *Nature medicine*. 2011;16:535-543, 531p following 143
8. Wang Y, Krishna S, Golledge J. The calcium chloride-induced rodent model of abdominal aortic aneurysm. *Atherosclerosis*. 2013;226:29-39
9. Patel V, Li L, Cobo-Stark P, Shao X, Somlo S, Lin F, Igarashi P. Acute kidney injury and aberrant planar cell polarity induce cyst formation in mice lacking renal cilia. *Human molecular genetics*. 2008;17:1578-1590
10. Lanoix J, D'Agati V, Szabolcs M, Trudel M. Dysregulation of cellular proliferation and apoptosis mediates human autosomal dominant polycystic kidney disease (adpkd). *Oncogene*. 1996;13:1153-1160
11. AbouAlaiwi WA, Ratnam S, Booth RL, Shah JV, Nauli SM. Endothelial cells from humans and mice with polycystic kidney disease are characterized by polyploidy and chromosome segregation defects through survivin down-regulation. *Human molecular genetics*. 2011;20:354-367
12. Nauli SM, Alenghat FJ, Luo Y, Williams E, Vassilev P, Li X, Elia AE, Lu W, Brown EM, Quinn SJ, Ingber DE, Zhou J. Polycystins 1 and 2 mediate mechanosensation in the primary cilium of kidney cells. *Nature genetics*. 2003;33:129-137
13. AbouAlaiwi WA, Takahashi M, Mell BR, Jones TJ, Ratnam S, Kolb RJ, Nauli SM. Ciliary polycystin-2 is a mechanosensitive calcium channel involved in nitric oxide signaling cascades. *Circulation research*. 2009;104:860-869
14. Nauli SM, Kawanabe Y, Kaminski JJ, Pearce WJ, Ingber DE, Zhou J. Endothelial cilia are fluid shear sensors that regulate calcium signaling and nitric oxide production through polycystin-1. *Circulation*. 2008;117:1161-1171

15. Abdul-Majeed S, Nauli SM. Dopamine receptor type 5 in the primary cilia has dual chemo- and mechano-sensory roles. *Hypertension*. 2011;58:325-331
16. Amores A, Postlethwait JH. Banded chromosomes and the zebrafish karyotype. *Methods in cell biology*. 1999;60:323-338
17. Rothschild SC, Francescatto L, Drummond IA, Tombes RM. Camk-ii is a pkd2 target that promotes pronephric kidney development and stabilizes cilia. *Development*. 2011;138:3387-3397
18. Obara T, Mangos S, Liu Y, Zhao J, Wiessner S, Kramer-Zucker AG, Olale F, Schier AF, Drummond IA. Polycystin-2 immunolocalization and function in zebrafish. *J Am Soc Nephrol*. 2006;17:2706-2718
19. Sun Z, Amsterdam A, Pazour GJ, Cole DG, Miller MS, Hopkins N. A genetic screen in zebrafish identifies cilia genes as a principal cause of cystic kidney. *Development*. 2004;131:4085-4093

SUPPLEMENTAL MOVIE LEGENDS

Movie S1. Normal cell division in renal epithelial cell.

The movie shows a cell undergoing a normal mitotic event. The movie was analyzed by superimposing DIC and Hoechst fluorescence images, which were taken every five minutes with 40X magnification.

Movie S2. Failure of cytokinesis induced polyploidy formation in survivin knockdown renal epithelial cell.

The movie shows that abnormal cytokinesis leads to polyploidy formation. The survivin knockdown cell is able to initiate cell division but is unable to execute cytokinesis properly. The cell then shows various membrane blebbing followed by the formation of a cytomegalic cell with multiple nuclei. Images were captured every two minutes with 40X magnification.

Movie S3. Normal cell division in vascular endothelial cell.

The movie shows a cell undergoing a normal mitotic event. The movie was analyzed by superimposing DIC and Hoechst fluorescence images, which were taken every two minutes with 40X magnification.

Movie S4. Failure of cytokinesis induced polyploidy formation in survivin knockdown vascular endothelial cell.

The movie shows that abnormal cytokinesis leads to polyploidy formation. The survivin knockdown cell is able to initiate cell division but is unable to execute cytokinesis properly. The cell then shows various membrane blebbing followed by the formation of a cytomegalic cell with

multiple nuclei. Of note is the presence of another multinucleated cell within the field of view. Images were captured every two minutes with 40X magnification.